Toward a Miniaturized Wireless Fluorescence-Based Diagnostic Imaging System

Moussa Kfouri, Ognian Marinov, Paul Quevedo, Naser Faramarzpour, *Student Member, IEEE*,
Shahram Shirani, *Senior Member, IEEE*, Louis W.-C. Liu, Qiyin Fang, *Member, IEEE*,
and M. Jamal Deen, *Fellow, IEEE*

Abstract—Fluorescence-based spectroscopy and imaging techniques provide qualitative and quantitative diagnostic information on biological systems. In this paper, we report on the design, fabrication, and testing of a miniaturized wireless fluorescence imaging device for noninvasive clinical diagnosis and screening of diseases in the gastrointestinal tract. The system includes three submodules: optical imaging, electronics control and image acquisition, and information processing and transmission. These modules were individually developed and tested before being integrated into a battery-powered wireless device. The final integrated system is mounted in a customized, compact cylindrical housing. The performance of each individual module and the overall integrated system has been evaluated using fluorescent phantoms. It has been demonstrated that the miniaturized device can acquire spectrally resolved fluorescence images and transmit the image stream wirelessly. An important outcome of this feasibility study is the identification of important technological issues and pathways for future prototype development.

Index Terms—Encapsulated endoscopy, fluorescence imaging, gastrointestinal (GI) tract, noninvasive diagnosis, wireless.

I. INTRODUCTION

CATHETER-BASED video endoscopy, in which a ∼2 cm diameter tube containing fiber optic cables carrying visible light is inserted into the gastrointestinal (GI) tract of a patient, is one of the most widely used methods for GI cancer screening and diagnosis. Although catheter-based endoscopy provides useful diagnostic information, it has been documented that the procedure is relatively invasive and costly due to the need of specialized equipments, operating suites, as well as the presence of an endoscopist to administer the procedure [1].

Alternatives that exclude the use of a catheter have recently been investigated and developed. These techniques use in-gestible capsule-size cameras, typically the size of a large vitamin pill, to provide visible illumination and acquire the images of the GI tract. The most publicized capsule is the PillCam (previously marketed as M2A) capsule by Given Imaging [2]. These capsules were developed to challenge push enteroscopy and radiology in diagnosing diseases usually found in the GI tract: diseases such as obscure bleeding, irritable bowel syndrome, Crohn's disease, and chronic diarrhea [3].

Typical wireless imaging capsules are about 11 mm (diameter) × 30 mm (length) and consist of an optical dome, a focusing lens, white light illumination LEDs, batteries, a wireless transmitter with antenna, and a CMOS imager. The images are captured over a 7–8 h period inside the GI tract, and then, transmitted using UHF-band radio-telemetry to aerials attached to the patient's body using a waist belt that also contains electronic memory for storing the received video images. Propelled by peristalsis, the pill travels through the GI tract without noticeable discomfort, and no air inflation is required [3]–[5].

The capsule's ability to visualize most of the small bowel mucosa in the small intestine in a convenient and safe manner highlights it as an appealing diagnostic method. When compared to push enteroscopy, the wireless imaging pill demonstrated 71% superior diagnostic yield [2], and the procedure is noninvasive. However, conventional visible light images are not always sufficient for detecting cancer at early stages [6]–[8], when treatment is usually more successful. Additionally, a gastroenterologist is required to interpret and evaluate all the 7–8 h of video in order to identify potential sites of malignancies, which is lengthy and costly for screening applications.

When biological tissue is illuminated by UV light, endogenous tissue fluorescence (also known as autofluorescence) may be observed in the 380–600 nm range. The emitted fluorescence light contains biochemical and physiological information of the targeted tissue, and hence, can be used for diagnosis based on the differences in spectroscopic features. Additional contrast may be achieved by administering exogenous fluorophores prior to tissue examination [9]. Diagnostic techniques based on fluorescence spectroscopy and imaging have been extensively investigated over the past 20 years [10]. These techniques usually require complex high-sensitivity photodetection systems and complex electronic systems for control, data processing, and communication [10]–[12].

Irradiation of the GI tract tissue with UV light and the detection of emitted fluorescence have been reported to provide better information for earlier detection of cancer [7], [8]. A catheter-based instrument [light induced fluorescence endoscopy–GI

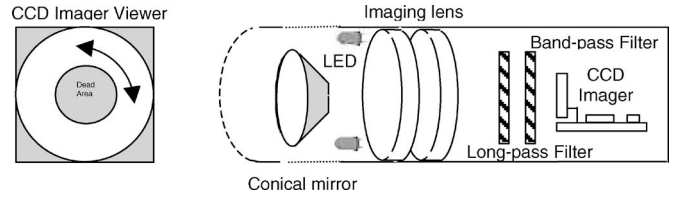Fig. 1. Conceptual design of the wireless fluorescence imaging system for noninvasive clinical diagnosis.

Fig. 2. Schematic showing the optical imaging module (right) and field of view on the CCD imaging sensor (left). UV excitation is achieved via the 360 nm LEDs. Side view fluorescence images are projected to the CCD through the conical mirror and two imaging lenses. A long-wavelength-pass filter is used to block scattered excitation light, while spectral band selection is achieved using the narrow bandpass filter placed in front of the CCD.

(LIFE–GI) tract] has been subsequently developed to demonstrate the effectiveness of this approach by Xillix [13]. This instrument provides real-time video images of tissue autofluorescence at two spectral bands using a fiber optic endoscope with light sources and detection systems in the proximal end of the scope. Conventional white light images are also acquired in a different imaging channel, and are superimposed on the fluorescence images. Studies have shown that abnormal tissues displayed significant decrease in fluorescence intensity along with an increase in the ratio of red-to-green fluorescence. Dysplastic or neoplastic areas appear reddish due to a higher red-to-green ratio, while other areas appear cyan [14]. Additionally, our preliminary results using macroscale spectroscopy systems have indicated that autofluorescence signals from inflamed tissues are different from normal tissues.

The decrease in autofluorescence in preinvasive tissue is believed to be from three different sources: 1) decrease in fluorophore amount or quantum yield within the tissue, 2) the changes in tissue architecture, and 3) the increase in blood volume due to the increase in the microvascular density [14]. These quantitative features may enable a "smart" diagnostic method that allows an artificial intelligent system to prescreen the images, which may significantly reduce the time required for a gastroenterologist to interpret the data. However, the invasiveness of catheter-based systems calls for the design of a noninvasive, more convenient system similar to the PillCam capsule that can combine the advantages of both systems into one device.

In this paper, we describe the design, implementation, and performance evaluation of a proof-of-concept miniaturized fluorescent imaging system, as a first step toward a fully integrated wireless, noninvasive imaging system for the detection of cancer in the GI tract.

II. DESIGN AND IMPLEMENTATION

The conceptual design of the encapsulated wireless fluorescence imaging device is shown in Fig. 1. It consists of three subsystems: an optical imaging module, an electronic image acquisition module, and an image processing and wireless communication module. The optical imaging module provides illumination and collection of florescence light with desired spectral features. The image is acquired using a high-sensitivity camera system, and then, processed and transmitted to an external receiver. Initially, the three modules were separately developed, and then, integrated into one prototype. Details of the design and implementation of each module are discussed, respectively, in Sections II-A, II-B, and II-C.

A. Optical Imaging Module

The optical imaging system was designed to deliver the excitation UV light to the targeted tissue and collect the induced fluorescent light in a desired spectral band. The schematic diagram of the optical module is shown in Fig. 2. A set of eight LEDs arranged in a circle in front of the imaging lenses were used for illumination. Four of the LEDs were UV emitting at 360 nm for fluorescence excitation and the other four were normal white light (400–700 nm) LEDs for conventional video endoscopy. The illumination light is reflected by a customized conical mirror and projected to the sidewall of the GI tract. Autofluorescence emitted from the tissue is collected by the same mirror and two achromatic imaging lenses, and then, projected onto a high-sensitivity charge-coupled device (CCD) imager. A 0–2 mm variable diameter aperture is inserted between the two lenses to control the depth of view. A long-pass filter (WB380, Optima, Inc., Tokyo, Japan) is used to block the scattered excitation light from reaching the CCD imager. Spectral selection of the fluorescence light is achieved using a narrow bandwidth bandpass filter at the desired wavelength. The intensity of the excitation light is typically three to four orders of magnitude higher than that of the emitted fluorescence light. Therefore, one of the main design considerations is to minimize the scattered excitation light from reaching the CCD. This is achieved by positioning both filters as close to the CCD imager as possible and using plastic imaging lens with low UV transmission.

Two types of UV LEDs for fluorescence excitation sources were evaluated. The first type is a high-power UV LED with peak wavelength of 365 nm, and optical output power of up to 100 mW at 500 mA input current. The second type is a low-power UV LED with the same peak wavelength as the first type, but with an optical power output of 2 mW at 20 mA of bias current. In the initial tests, the high-power LED's power consumption was found to be too high for battery-powered wireless devices, and it also caused excess heating of the device, thus prohibiting its use in clinical environments. Experiments
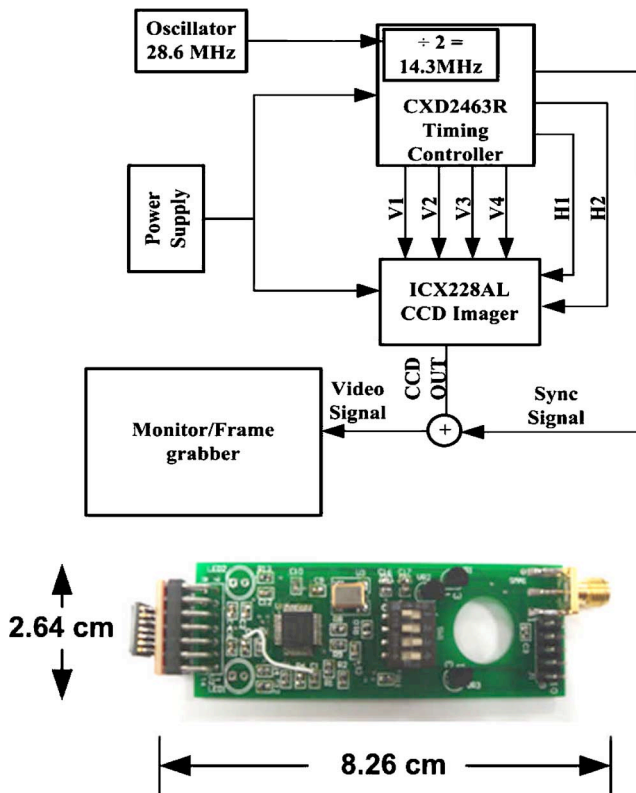
Fig. 3. Schematic and photograph of the image acquisition module. A block diagram showing the flow of signals between the imager and the timing controller in the electronic imaging system (top) and a picture of the prototype of the imaging acquisition module (bottom). The CCD imager is on the left mounted perpendicular to the PCB.
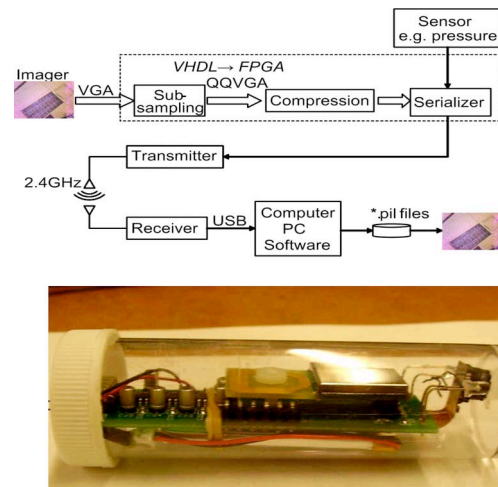

Fig. 4. Data flow diagram of the wireless imaging/sensing system (upper) and a photograph of the encapsulated prototype mounted in a custom housing (bottom).

showed that the low-power LEDs (second type) can provide sufficient UV excitation to induce fluorescence in our tests while maintaining manageable levels of power consumption and heat generation. Therefore, these LEDs were chosen for use in the prototype system, where all subsequent tests were performed. Lower intensity illumination, however, resulted in lower emission intensity, which, in turn, led to reduced signal-to-noise levels in the acquired fluorescence images.

B. Electronic Image Acquisition Module

The image acquisition module was optimized for high-sensitivity detection. The power consumption and size were minimized using off-the-shelf commercial components. A schematic of the signal flow is shown in Fig. 3.

A diagonal one-fourth of an inch interline monochromatic CCD sensor (ICX228AL from Sony) was used for image acquisition. The CCD imager only provides the video signal output without any type of synchronization signal needed by the image acquisition modules. It was, therefore, necessary to invert the video signal; then to use a summing amplifier configuration to add the synchronization signal obtained from a timing controller to the video signal.

A 48-pin timing controller (CXD2463R, Sony) was used to provide the clocking signals for the vertical and horizontal registers of the imager. This CMOS IC generated the synchroniza-

tion signal and provided electronic shutter as well as window pulse outputs for backlight compensation. It also supported different external synchronization modes with automatic external synchronization discrimination, a useful feature when used in combination with pulsed excitation light. The timing controller was clocked by a 28.6363 MHz crystal oscillator, and a DIP switch was used to change the electronic shutter speed. A dual wideband, low-noise, 160 MHz operational amplifier was used, as well as a signal processing IC (CXA1310AQ, Sony) customized for compact and low-power consumption applications. This configuration is also equipped with built-in image processing functions such as a wide variable automatic gain control (AGC, 4–32 dB), built-in amplification, and an adjustable white (saturation) level for wide dynamic range (140 IRE). The final processed analog video signal was then fed out to the wireless image transmission module.

All the components were mounted on a 2.64 cm × 8.26 cm four-layer printed circuit board (PCB), shown in Fig. 3. The CCD imager was placed at 90° angle from the board, pointing forward toward the optical module.

C. Wireless Transmission Module

Wireless data transmission from endoscopic capsules is usually quite challenging in practice. Issues such as mismatch in information volumes, restrictions for power consumption and size must be adequately addressed in the context of the application. We have explored several possible solutions to meet these challenges. The RF wireless communication system was designed, and a prototype system with off-the-shelf components was fabricated on the same PCB as the image acquisition module. A block diagram of the design is depicted in Fig. 4. An off-the-shelf RF communication link (transmitter and receiver) was used for prototyping purposes. The power consumption of the system is sufficiently low such that it can be completely powered by a single Li-ion battery.

Due to the use of high-resolution CCD imager, the image data volume as acquired by the imager is larger than the current bandwidth constraints for wireless data transfer. For example, a video graphics array (VGA) image frame consists of 640 columns $\times$ 480 rows, which is equivalent to 307 200 pixels, each corresponding to 2 Bytes and resulting in 614 400 Bytes/frame, or approximately, 5 Mbits/frame. On the other hand, wide-band wireless communications is limited to 1 Mbits/s, or it will take 5–10 s per image frame if one tries to transmit a VGA image directly by wireless communications. Therefore, as shown by the data flow in Fig. 4, the VGA images are subsampled to quarter–quarter VGA (QQVGA), which reduces the image volume by 16 times, and then, data compression is applied to achieve additional reduction of 4 times. Thus, the volume of the compressed image frame was reduced to about 10–12 kBytes, allowing us to include correction codes and other useful information, but still having frame data volume below 100 kbits/frame. The data from the compressed images are combined in the serializer, which feeds the RF transmitter at a rate of 250 kbits/s, and the RF link forwards the data to a host computer with an acceptable data loss of 10% that can be recovered in real time using the correction codes mentioned before. All functions in the flow diagram of Fig. 4 were performed in real time, from image acquisition through compression, transmission, receiving and storing, to decoding and visualization of video stream on the host computer. The power consumption of the module was also sufficiently low such that all the aforementioned procedures can be operated using battery power.

The prototypes for the different modules of the wireless fluorescence imaging system were tested, and they functioned as desired. A custom cylindrical housing (2 cm in diameter and 10 cm long) was designed, and the entire wireless imaging system including the wireless transmitter was integrated as shown in Fig. 4 and tested in free space.

III. RESULTS

The emission spectral features and output power of the UV LEDs were first characterized. The emission spectra were measured by a calibrated fiber optics spectrometer (OSM400, Newport, Irvin, CA). As shown in Fig. 5(a), the LEDs exhibited a symmetrical Gaussian-like profile peaking around 370 nm with a full-width at half-maximum (FWHM) bandwidth of $\sim$10 nm. It was noticed that the output intensity decreases considerably soon after powering-on the device, and then, it stabilizes after 30 s, most likely influenced by the device's thermal transient.

There were observable variations of the emission spectrum as well as the spectral bandwidth at different input current settings. As shown in Fig. 5(b), the peak of the emission spectrum displayed significant redshift as the intensity was higher. Similarly, the bandwidth of the emission spectrum also increases slightly from 8 to 11 nm as the current/intensity increases, as shown in Fig. 5(c). The changes in spectral emission features may be attributed to the changes of the materials characteristics with the rise of temperature accompanying the input current increase. Overall, these changes are minor compared with the relatively broad absorption band of the typical tissue fluorescence com-

ponents such as collagen and lipids. However, they should be considered while choosing an appropriate long-wavelength-pass filter to suppress backscattered excitation light. In our system, a 380 nm cutoff filter was chosen to reduce the transmission of the excitation light at low current, which corresponds to a 360 nm peak. For high current use, e.g., at 370 nm emission peak, a 400-nm-long wavelength pass filter may be required to sufficiently suppress the backscattered excitation light.

The output power was measured using an optical power meter (1830 C, Newport) with a visible-light detector head (818-SL/CM, Newport). The measurements were performed 60 s after the LEDs were powered on, so they were thermally stabilized. It has been shown in Fig. 5(d) that the output power increases linearly with the input current up to 500 mA, the manufacturer's specified maximum operating current.

The acquired image is spatially distorted by the conical mirror, as shown in Fig. 6. The spatial resolution of the distorted image becomes worse when regions closer to the apex of the cone were used. Therefore, only the outer region of the image may be used, and the apex of the conical mirror is reserved for a future forward imaging channel. The distorted image was subsequently unwrapped in the final image processing module by using a polar-to-rectangular coordinate transformation. This filter reads the image as if it were plotted on polar coordinates, then replots each pixel onto a cartesian plane. The comparison between the initial distorted image and the unwrapped image is shown in Fig. 6.

After integrating the optical system and the electronic imaging modules, proof-of-concept tests were conducted on the completed endoscopic fluorescence imaging system using fluorescent phantoms. The first phantom is a piece of paper containing texts printed in black ink and two fluorescent lines (one green, one red). As shown in Fig. 7(a), when first illuminated by the white light without a bandwidth filter in front of the CCD, both the printed text and the green fluorescence mark are visible in the acquired image. When the UV LED was used as the illumination source along with a bandpass filter (600 $\pm$ 40 nm), as shown in Fig. 7(b), both the green and red fluorescence marks were visible, while the printed text was not. This test simulated lesions that are not visible under regular white light endoscopic imaging, but can be detected using UV illumination and spectrally selected imaging. Further tests using fresh porcine skin stained with fluorescence dyes, shown in Fig. 7(c) and (d), have demonstrated that this prototype system can also selectively image the features that are only available in a particular spectral band.

The wireless transmission module was tested and functioned as expected. The restrictions on device size and power consumption were key design constraints to be minimized. These restrictions required innovative approaches for image compression and wide-band short-range RF transmission in order to overcome several drawbacks. In order to transmit the images in real time, data compression has to be performed. However, it is well established that image compression by a factor greater than 2 would result in significant loss of image quality [15]. Compression algorithms also require extensive computation, usually accompanied with increased power consumption [16], which is
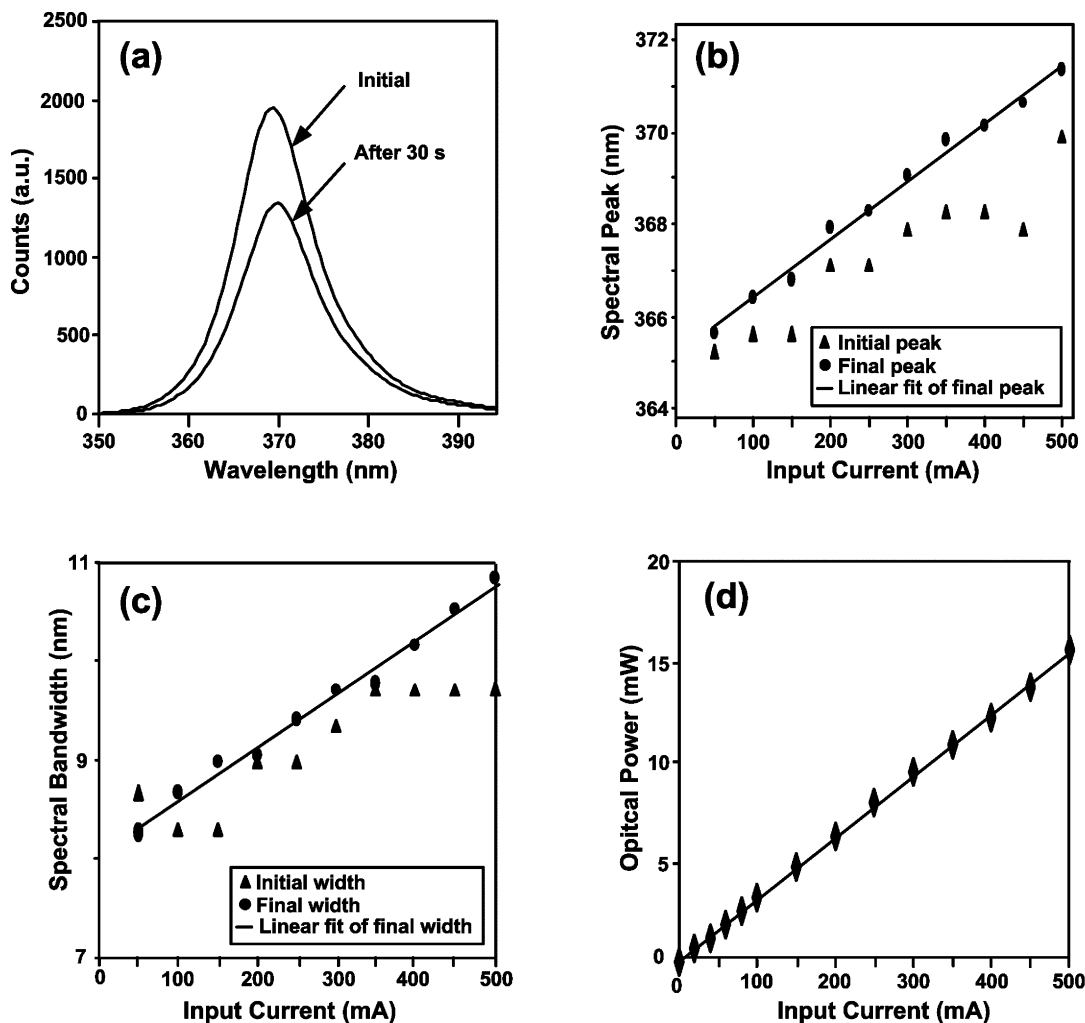
Fig. 5. Emission spectra and optical power measurements of the low power UV LED. (a) Emission spectra of the UV LED. It was noticed that the intensity decreases considerably after powering on the device for 30 s, and then, stabilizes probably due to the device's thermal stability. (b) Peak of the emission spectra vs. input current, where the initial bandwidth was measured within 5 s the LED was loaded with desired current, and the final bandwidth was measured after 30 s the LED was loaded and is thermally stable. (c) Bandwidth of the emission spectra vs. input electrical current, where the initial and final measurements were done similar to those described in (b). (d) Optical output power vs. the input electrical current. All measurements in (b)–(d) at different input current were performed when the LEDs were completly cooled to room temperature before the next measurement.

Fig. 6. Image distortion due to the conic mirror and software image reconstruction. Left: unprocessed image acquired through the side-looking optical imaging system; center: corresponding unwrapped image; right: illustration of the original unprocessed image and corresponding reflective surface on the conic mirror. The spatial resolution is degraded at the tip of the conical mirror (center portion of the original image on the left, top portion of the reconstructed image in the middle).

not desirable for a wireless device. To get insight into the trade-off between compression and quality, we have employed differential variable length coding in the image compression, and then, we changed the image targets so that the effective level of compression also changes. The results are shown in Fig. 8.

It is interesting to observe that the trend shown in Fig. 8 is the opposite of what one would naturally expect. In particular,

the image quality decreases when the data compression is lower and the average length of the code word is longer, whereas the quality increases when the code words are shorter and the data compression rate is higher. Intuitively, one may expect the opposite: low quality at high compression and vice versa. This inverse dependence between transmitted image quality and data compression rate is a typical artifact for wireless imaging systems,
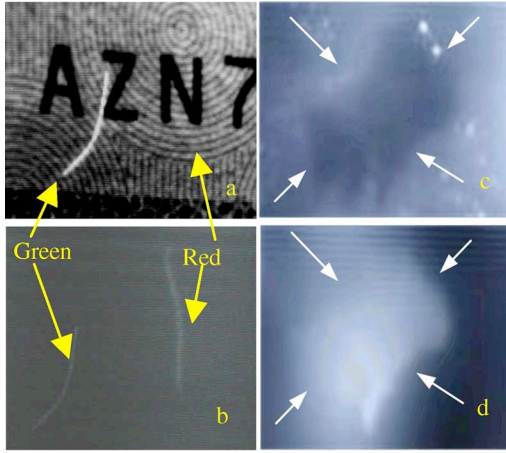
Fig. 7. Images of fluorescent phantoms acquired by the proof-of-concept system. The spectral selection is achieved through placing a bandpass filter (600 ± 40 nm) in front of the CCD imager. Left: a paper-based phantom containing both printed text and two fluorescent lines (green: 550 nm and red: 620 nm). (a) Illuminated by the white light LED without the bandpass filter (top left). (b) Illuminated by the UV LED illumination with the bandpass filter (bottom-left). Under white light illumination in (a), only the green fluorescent line is visible along with the text. The red fluorescent line is visible only under UV illumination, shown in (b). Right: fresh porcine skin stained with fluorescein. (c) Illuminated by the white light LED without the bandpass filter (top right). (d) Illuminated by the UV LED with the bandpass filter (bottom right). Under white light illumination, the stained area (indicated by the area surrounded by the arrows) appears dark. Under UV illumination and with appropriate filters, only the stained area was highlighted.
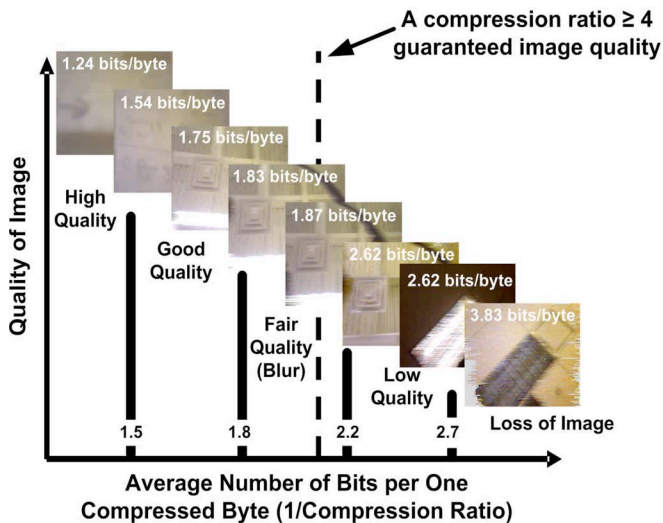

Fig. 8. Dependence of image quality on the average length of the code words used in image compression. The tradeoff between compression and image quality is reversed in wireless system with limited bandwidth. At high compression ratio, when the code words are short, less than 2 bits per uncompressed byte, the quality of the received images in the video stream is good. On the contrary, the image quality decreases when the code words are longer than 2.2 bits per uncompressed byte, and an image loss occurs when the code words are longer than 3 bits.

in which the data transfer rate is limited by the RF link. Thus, the image compression in these systems is chosen such that the RF link would not be overloaded. In commercial systems, compression schemes are chosen after a difficult decision in the tradeoff between image quality, power consumption, and

loss of information in the RF link. Due to the scattering of both excitation and emission photons, wide-field fluorescence imaging on the tissue level usually has relatively low spatial resolution compared to conventional imaging. Therefore, on-chip hardware binning of the imager pixels may significantly reduce the requirement for data compression. Further investigation via *in vitro* testing on phantoms or on *ex vivo* tissue are, therefore, required to quantitatively determine these tradeoffs.

IV. DISCUSSION

Fluorescence-imaging-based wireless endoscopy has two main advantages over current catheter-based techniques for screening and diagnostic applications in the GI tract. First, it is noninvasive and does not need to be administered by a specialist. Second, the functional diagnostic information provided by a fluorescence signal may enable automated artificial intelligence programs to process the large amount of images acquired during the 7–8 h period.

The acquisition of spectrally resolved fluorescence images requires complex and usually bulky optical and electronics instrumentation. To design a wireless system that can be used for GI tract diagnosis, the main challenges include miniaturization of both optical and electronic components as well as minimization of power consumption.

Most of the optical and electronics parts used to build the prototype are commercially available, off-the-shelf components. Although it is a compact system (2 cm in diameter and 10 cm in length), the integrated prototype is still too large to be practical in a clinical environment. Further miniaturization toward a practical prototype may be achieved through the use of customized electrical components such as custom-designed ICs for both imaging acquisition and wireless communications on the same chip. As for the optical module, miniaturization of the individual components as well as the overall system size is more challenging. For example, efficient tunable spectral selection for the whole field is highly desired, but it would be very difficult to miniaturize for the current bandpass-filter-based system. Therefore, advanced multispectral imaging technologies need to be investigated such as acoustooptical tunable filters and/or liquid crystal tunable filters. The current device is running on battery power. In practice, coupling power wirelessly from outside the body to the system inside would be preferred.

The current prototype uses a separate CCD imager chip. A CCD imager has acceptable noise performance and offers high sensitivity. However, further miniaturization of the system is not possible unless a CMOS imager is used. This is because the CCD technology is not compatible with mainstream CMOS IC technology, and the cost of integrating a CCD with CMOS electronics would be much higher than a custom-designed CMOS imaging and electronics system. By using CMOS technology, the rest of the electronic components of the system, including the RF communication module, can be fabricated on the same chip with the imager. This will reduce the size of the system, its power consumption, and the price of the finished product [17].

For fluorescence imaging systems, the imager should have high sensitivity and high dynamic range. It should also be able
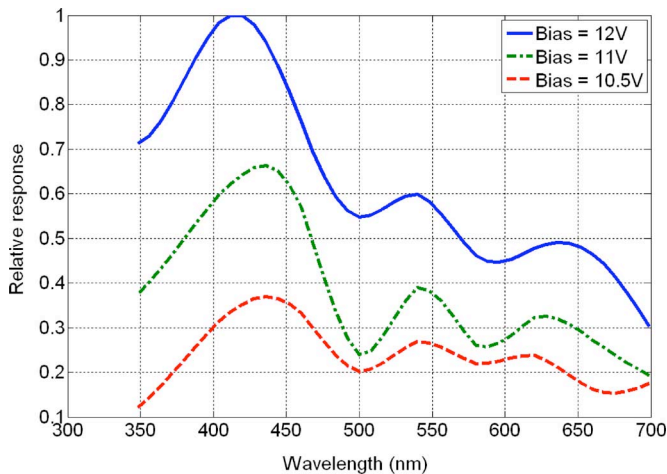
Fig. 9. Measured relative spectral response of our APD at three reverse bias voltages. This APD was fabricated in a 0.18 μm CMOS technology. Note that the relative spectral response stays approximately the same, independent of reverse bias voltage. Also, the APD has high responsivity around blue and UV, which is due to the ultrashallow implanted junctions of the modern CMOS technology.

to detect light of short wavelengths. Modern CMOS photodetectors are reported that can achieve these requirements [18], [19]. Considering the pixel structure of CMOS imagers, they cannot offer as high resolutions as do CCD imagers. However, the requirement on resolution in our application is not critical, and the required resolution can easily be achieved using imagers fabricated in modern submicron CMOS technologies.

The active pixel sensor (APS) is a widely used pixel structure for CMOS imagers. The APS has a simple structure with wide dynamic range. However, it cannot offer both high sensitivity and fast speed due to its integrating mode of operation. To improve the sensitivity of existing APS using the commonly used pixel structure, we recently proposed a dc level output technique [18], [19]. The new mode of reading the output was shown [18], [19] to be about 30 times better than the conventional reading mode using the swing output.

For imagers with both high sensitivity and fast response characteristics, avalanche photodiodes (APDs) can be used. The APDs have the ability of fast detection of very low levels of light due to their intrinsic gain and short carrier transit time. Using an APD array for our prototype will reduce the power of UV illumination by the light source, as the APD can detect lower levels of fluorescence emission. This will decrease the UV light exposure to the patient and also reduce the consumed power by the UV LEDs of the device. We have designed and fabricated Geiger-mode APDs with active quench and reset peripheral circuitry in 0.18 μm CMOS technology [20]. These APDs are made with shallow junctions that can detect blue and UV light. Fig. 9 shows the relative spectral response of our APD. In Fig. 9, it can be seen that the relative response of the APD changes with the applied bias due to changes in the multiplication within the diode. However, the relative spectral response stays approximately the same. The APD has high responsivity around blue and UV, which is due to the ultrashallow implanted junctions of the modern CMOS technology. Because of this

good responsivity at shorter wavelengths, such an APD would be very suitable for UV fluorescence imaging applications. Finally, because these APDs were designed and fabricated in a commercial CMOS technology, integrating a 2-D APD-based imager with other electronic circuitry would be feasible because of low cost, and the power consumption would be much less than the existing CCD-based imager and separate chips for control, processing, and wireless communications.

V. CONCLUSION

In this paper, we reported on the development of a prototype wireless fluorescence imaging system for noninvasive GI endosopy. The prototype contains three modules, which were first developed and tested individually, and then, integrated as a complete system. Initial characterization and proof-of-principle testing on fluorescent phantoms have demonstrated that this prototype system is capable of acquiring and analyzing fluorescence images at desired spectral bands while operating wirelessly.

Research on multimodality embedded sensor modules, such as temperature, pH, and ion-selective sensors, is currently ongoing. Also, methods of accurately locating the pill inside the GI tract remains a challenge in the field of capsule endoscopy. On another level, particular attention should be devoted to data acquisition--storage, data logging, synchronization, linking, and control--image recognition algorithms for "smart diagnosis," and fabrication technologies for biomedical applications and environmental monitoring.

REFERENCES

[1] M. B. Wallace, V. L. Durkalski, J. Vaughan, Y. Y. Palesch, E. D. Libby, P. S. Jowell, N. J. Nickl, S. M. Schutz, J. W. Leung, and P. B. Cotton, "Age and alarm symptoms do not predict endoscopic findings among patients with dyspepsia: A multicentre database study," *Gut*, vol. 49, pp. 29–34, 2001.

[2] M. Yu, "M2A$^{\mathrm{TM}}$ capsule endoscopy: A breakthrough diagnostic tool for small intestine imaging," *Gastrenterol. Nurs.*, vol. 25, no. 1, pp. 24–27, 2002.

[3] D. S. Mishkin, R. Chuttani, J. Croffie, J. DiSario, J. Liu, R. Shah, L. Somogyi, W. Tierney, L. M. W. K. Song, and B. T. Petersen, "ASGE technology status evaluation report: Wireless capsule endoscopy," *Gastrointest. Endosc.*, vol. 63, no. 4, pp. 539–545, 2006.

[4] K. Arshak, E. Jafer, G. Lyons, D. Morris, and O. Korostynska, "A review of low-power wireless sensor microsystems for biomedical capsule diagnosis," *Microelectron. Int.*, vol. 21, no. 3, pp. 8–19, 2004.

[5] E. A. Johannessen, L. Wang, C. Wyse, D. R. S. Cumming, and J. Cooper, "Biocompatibility of a lab-on-a-pill sensor in artificial gastrointestinal environments," *IEEE Trans. Biomed. Eng.*, vol. 53, no. 11, pp. 2333–2340, Nov. 2006.

[6] C. Arens, T. Dreyer, H. Glanz, and K. Malzahn, "Indirect autofluorescence laryngoscopy in the diagnosis of laryngeal cancer and its precursor lesions," *Eur. Arch. Oto-Rhino-Laryngol.*, vol. 261, no. 2, pp. 71–76, 2004.

[7] B. Chwirot, S. Chwirot, W. Jedrzejczyk, M. Jackowski, A. Raczynska, J. Winczakiewicz, and J. Dobber, "Ultraviolet laser-induced fluorescence of human stomach tissues: Detection of cancer tissues by imaging techniques," *Lasers Surg. Med.*, vol. 21, pp. 149–158, 1998.

[8] P. J. M. George, "Fluorescence bronchoscopy for the early detection of lung cancer," *Thorax*, vol. 54, pp. 180–183, 1999.

[9] A. Bogaards, A. Varma, S. P. Collens, A. Lin, A. Giles, V. Yang, J. M. Bilbao, L. D. Lilge, P. J. Muller, and B. C. Wilson, "Increased brain tumor resection using fluorescence image guidance in a preclinical model," *Lasers Surg. Med.*, vol. 35, pp. 181–190, 2004.

[10] R. Richards-Kortum and E. Sevick-Muraca, "Quantitative optical spectroscopy for tissue diagnosis," *Annu. Rev. Phys. Chem.*, vol. 47, pp. 555–606, 1996.

[11] B. Jaggi, M. J. Deen, and B. Palcic, "Design of a solid state microscope," *Opt. Eng.*, vol. 28, no. 6, pp. 675–682, Jun. 1989.

[12] B. Jaggi, M. J. Deen, and B. Palcic, "Solid state microscope," Canadian Patent 1 304 612, Jul. 7, 1992.

[13] H. Zeng, A. Weiss, R. Cline, and C. E. MacAulay, "Real-time endoscopic fluorescence imaging for early cancer detection in the gastrointestinal tract," *Bioimaging*, vol. 6, pp. 151–165, 1998.

[14] H. Zeng, C. MacAulay, S. Lam, and B. Palcic, "Light induced fluorescence endoscopy (LIFE) imaging system for early cancer detection," *Proc. SPIE*, vol. 3863, pp. 275–282, 1999.

[15] A. Shoham and J. Bier, "Introduction to video compression," Berkeley Des. Technol., San Francisco, CA, Tech. Rep., Mar. 2004.

[16] X. Xie, G. Li, X. Chen, X. Li, and Z. Wang, "A low-power digital IC design inside the wireless endoscopic capsule," *IEEE J. Solid-State Circuit*, vol. 41, no. 11, pp. 2390–2400, Nov. 2006.

[17] M. Willemin, N. Blanc, G. K. Lang, S. Lauxtemann, P. Schwider, P. Seitz, and M. Wany, "Optical characterization methods for solid-state image sensors," *Opt. Lasers Eng.*, vol. 36, no. 2, pp. 185–194, 2001.

[18] N. Faramarzpour, M. J. Deen, and S. Shirani, "An approach to improve the signal-to-noise ratio of active pixel sensor for low-light-level applications," *IEEE Trans. Electron Devices*, vol. 53, no. 9, pp. 2384–2391, Sep. 2006.

[19] N. Faramarzpour, M. J. Deen, S. Shirani, Q. Fang, L. W. C. Liu, F. Campos, and J. W. Swart, "CMOS based active pixel for low-light-level detection: Analysis and measurements," *IEEE Trans. Electron Devices*, vol. 54, no. 12, pp. 3229–3237, Dec. 2007.

[20] N. Faramarzpour, M. J. Deen, S. Shirani, and Q. Fang, "Fully integrated single photon avalanche diode detector in standard CMOS 0.18 μm technology," *IEEE Trans. Electron Devices*, vol. 55, to be published.

Paul Quevedo was born in Toronto, ON, Canada, in 1986. He is currently working toward the Undergraduate degree in biomedical and electrical engineering from McMaster University, Hamilton, ON, Canada.

In 2006, he was involved in the development of a minimally invasive fluorescent imaging prototype for cancer detection in the gastrointestinal (GI) tract.

Mr. Quevedo received the Natural Sciences and Engineering Research Council (NSERC) scholarship in 2007 to develop a model for DNA-based MOSFETs (BioFETs) in the cadence simulation environment.

Naser Faramarzpour (S'06) was born in 1980. He received the B.Sc. degree from Sharif University of Technology, Tehran, Iran, in 2002, and the M.Sc. degree in 2004 from McMaster University, Hamilton, ON, Canada, where he is currently working toward the Ph.D. degree, all in electrical engineering.

His current research interests include ultrasensitive photodetector design and device modeling.

Shahram Shirani (M'97–SM'04) received the B.Sc. degree in electrical engineering from Esfahan University of Technology, Isfahan, Iran, in 1989, the M.Sc. degree in biomedical engineering from Amirkabir University of Technology, Tehran, Iran, in 1994, and the Ph.D. degree in electrical and computer engineering from the University of British Columbia (UBC), Vancouver, Canada, BC, in 2000.

Since July 2000, he has been with the Department of Electrical and Computer Engineering, McMaster University, Hamilton, ON Canada, where he is currently an Associate Professor. His current research interests include image and video compression, imaging systems, multimedia communications, and ultrasonic imaging.

Dr. Shirani is a registered Professional Engineer.

Moussa Kfouri was born in Beirut, Lebanon, in 1983. He received the B.Eng. degree in computer engineering in 2005 from McMaster University, Hamilton, ON, Canada, where he is currently working toward the M.S. degree in electrical and computer engineering.

His current research interests include miniaturized minimally invasive imaging devices for clinical diagnosis and radio frequency analog integrated circuit design.

Ognian Marinov was born in Sofia, Bulgaria, in 1962. He received the M.Sc. and Ph.D. degrees in electronics from the Technical University, Sofia, Bulgaria, in 1986 and 1996, respectively.

In 1987, he joined the Faculty of Electronics, Technical University, Sofia. He was also with the École Nationale Supérieure de l'Électronique et de ses Applications (ENSEA), Cergy, France, in 1994 and 1995 and the Rheinisch-Westfälische Technische Hochschule (RWTH), Aachen, Germany, in 1998. Since 2000, he has been with McMaster University, Hamilton, ON, Canada. He was engaged in more than ten industrial and scientific projects on design and fabrication of measurement instruments, development of automatic test systems, characterization and modeling of electronic devices, design, fabrication, and implementation of sensors and systems for power network measurements, design of ICs, reliability and quality characterization, low-frequency noise, and characterization of polymeric electronic devices. He has authored or coauthored more than 25 papers. His current research interests include low-frequency noise in devices and breakdown, micropower circuit design, organic electronics, and technology and automation of measurements and characterization.

Louis W.-C. Liu was born in Hong Kong. He received the Bachelor's and Master's degrees in engineering physics, in 1988 and 1991, respectively, the Ph.D. degree in biomedical engineering, in 1996, and the M.D. degree, in 1998, all from McMaster University, Hamilton, ON Canada.

He completed his Internal Medicine Residency Training at the University of Toronto and his Gastroenterology subspecialty fellowship training at McMaster University. He is currently a practicing Gastroenterologist at the Toronto Western Hospital and an Assistant Professor of Medicine at the University of Toronto, Toronto, ON, Canada. He is currently receiving research funding from the Canadian Institute of Health Research (CIHR) and the Canadian Association of Gastroenterology. He has authored or coauthored 17 articles and three book chapters.

Dr. Liu is the recipient of the Clinician Scientist Award from the CIHR for the period between 2003 and 2007. Since 2002, he has been a Fellow of the Royal College of Physicians of Canada and licensed by the College of Physicians and Surgeons of Ontario and is currently a member of the American College of Gastroenterology, American Motility Society, Canadian Association of Gastroenterology, Canadian Association for the Study of the Liver, Canadian Medical Association, and the Ontario Association of Gastroenterology. He has received ten research awards; four of which were selected from international scientific meetings.

Qiyin Fang (M'01) received the B.S. degree in physics from Nankai University, Tianjin, China, in 1995, and the M.S. degree in applied physics and the Ph.D. degree in biomedical physics, in 1998 and 2002, respectively, from the East Carolina University, Greenville.

He is currently an Assistant Professor of engineering physics at McMaster University, Hamilton, ON, Canada and holds the Canada Research Chair in biophotonics. He was with the Minimally Invasive Surgical Technology Institute of Cedars-Sinai Medical Center, Los Angeles, first as a Postdoctoral Fellow and later as a Staff Research Scientist. His current research interests include optical spectroscopy and image guided minimally invasive diagnostic and therapeutic devices, miniaturized microoptoelectromechanical systems (MOEMS) sensors and imaging systems, and advanced optical microscopy and their emerging applications.

M. Jamal Deen (F'02) was born in Guyana, South America. He received the Ph.D. degree in electrical engineering and applied physics from the Case Western Reserve University, Cleveland, OH, in 1985.

He is currently a Professor of electrical and computer engineering, McMaster University, Hamilton, ON, Canada, where he is also the Senior Canada Research Chair in information technology and the elected Director of the Micro- and Nano-Systems Laboratory (MNSL). His current research interests include microelectronics/nanoelectronics and optoelectronics and their emerging applications. He was the Executive Editor of the *Fluctuations and Noise Letters* and a Member of the Editorial Boards of the *Journal of Nanoelectronics and Optoelectronics*, the *Microelectronics Journal*, the *Open Journal of Applied Physics*, and the *International Journal of High Speed Electronics and Systems*.

Dr. Deen was a Fulbright Scholar (under the Latin American scholarship program) from 1980 to 1982, an American Vacuum Society Scholar from 1983 to 1984, and a Natural Sciences and Engineering Research Council (NSERC) Senior Industrial Fellow during 1993. He was awarded the 2002 T.D. Callinan Award from the Electrochemical Society, a Humboldt Research Award from the Alexander von Humboldt Foundation in 2006, an International Business Machines (IBM) Faculty Award in 2006, and has won six Best Paper Awards. He is a Distinguished Lecturer of the IEEE Electron Device Society. He is currently the Editor of IEEE TRANSACTIONS ON ELECTRON DEVICES, He has been elected a Fellow of the Royal Society of Canada (FRSC), the Canadian Academy of Engineering (FCAE), the Institute of Electrical and Electronic Engineers (FIEEE), the Electrochemical Society (FECS), the American Association for the Advancement of Science (FAAAS), the Engineering Institute of Canada (FEIC), and Honorary Member of World Innovation Foundation-–the Foundation's highest honor.